Full Paper

Constant-Distance Mode Scanning Electrochemical Microscopy. Part II: High-Resolution SECM Imaging Employing Pt Nanoelectrodes as Miniaturized Scanning Probes

*Bernardo Ballesteros Katemann, Albert Schulte, Wolfgang Schuhmann**

Analytische Chemie – Elektroanalytik & Sensorik, Ruhr-Universität Bochum, Universitätsstr. 150, D-44780 Bochum, Germany
*e-mail: wolfgang.schuhmann@ruhr-uni-bochum.de

Received: June 2, 2003
Final version: July 31, 2003

Abstract
The potential of needle-type Pt disk nanoelectrodes as extremely miniaturized scanning probes for high resolution scanning electrochemical microscopy (SECM) was investigated. The accuracy of a piezoelectric shear-force based distance control allowed a precise positioning of the Pt nanoelectrodes in close proximity to the surface of interest not only in tip approach experiments but also throughout scanning and SECM imaging. As proof of the advanced quality of SECM imaging, high-resolution current and topography images of a three-dimensional LIGA microstructure will be presented both simultaneously acquired by operating Pt nanoelectrodes in the constant-distance mode of SECM.

Keywords: Scanning electrochemical microscopy (SECM), High resolution, Shear-force detection, Constant-distance mode, SECM tip, Nanoelectrode

1. Introduction

Merging the benefits of voltammetric microelectrodes with the ones of scanning probe techniques, scanning electrochemical microscopy (SECM) represents a powerful tool for studying local (electro) chemical properties of liquid/solid interfaces in their native environment [1–5]. In general, information's about the topography and discrete variations in conductivity and/or chemical reactivity are accessible at high spatial resolution from SECM measurements. With those, a mobile microelectrode (the SECM tip) is scanned in very close distance across the sample surface and its current response simultaneously monitored as a function of the x and y tip position. SECM imaging relies strongly on a dependence of the electrochemical tip response on the tip-to-sample distance (d) and the nature of the sample surface [6]. As a matter of fact, the achievable spatial resolution of SECM imaging is effectively related to the size of the microelectrodes used for scanning. Usually, disk-shaped metal or carbon microelectrodes with typical diameters of the active planar disk in the range of about 2–25 μm are used as scanning probes for imaging in the amperometric feedback or the generator/collector mode of SECM. Detailed information on the design and construction of such conventional SECM tips can be found in a recently published review [7].

Aiming on SECM imaging with sub-μm resolution, a lot of effort was focused on the fabrication of SECM tips with significantly reduced tip diameters and specially-designed electrodes with electrochemically active disks of nanometer dimensions ("nanoelectrodes") have recently been reported and proposed as potential scanning probes for high-resolution SECM [8–13]. However, to our knowledge only approach curve measurements and an early attempt to image a flat surface with a short scan range [8] using nanoelectrodes have been published until now. This might be explained by the extreme difficulties in operating a nanoelectrode as a scanning probe in the most often used constant-height mode of SECM. They arise due to the fact that the working distance appropriate for SECM imaging ought to be in the order of a few times the diameter of the active disk of the microelectrode used for scanning to make sure that the SECM tip is placed properly within the range of the modulation of the hemispherical diffusion profile in front of the electrode by the properties of the sample in the amperometric feedback mode or a good collection efficiency is guaranteed in the generator/collector mode. This implies that a nanoelectrode with, for instance, an effective radius of 100 nm has to be scanned at a distance of only about a few hundreds of nanometers above the specimen. Obviously, scanning SECM tips at such a small distance in constant height easily can lead to a tip crash or a loss of feedback when performed on tilted surfaces and no compensation for the surface tilt has been made (because of the extremely short tip-to-sample separation this is true even at very small tilt angles) or at surfaces that are featuring 3D structures with heights or grooves and holes with depths larger than a few times the diameter of the active disk of the nanoelectrodes themselves. For this reason and in order to avoid a tip crash or a loss of feedback it is a prerequisite for successful SECM imaging with nanometer-sized SECM tips to control accurately the tip-to-sample separation and SECM in a constant-distance mode of operation has to be used to force the SECM tip to follow the contours of the

  DOI: 10.1002/elan.200302918

sample surface during scanning. In addition to lowering the risk of damaging the tiny tips, constant-distance mode SECM with nanometer-sized scanning probes has the advantage that one obtains simultaneously information on both, the sample topography and its reactivity, which without any doubt will facilitate the interpretation of the SECM data.

First attempts to carefully control the tip-to-sample distance took advantage of so-called tip-modulation [14] and picking modes of SECM [15]. However, a clear convolution between distance and topology effects can only be gained by using non-electrochemical strategies for a concurrent and independent acquisition of the surface's topography and its local electrochemical properties. In 1995, we introduced such a non-electrochemical approach to SECM by exploiting a distance control with a shear-force based feedback mechanism [16] as originally developed by others for the positioning of ultra small optical fiber tips in scanning near field optical microscopy (SNOM) [17, 18]. The set-up with an integrated optical detection scheme for shear forces was successfully applied for surface modification [19], the positioning of non-amperometric SECM tips [20] and for measurements on soft biological samples, i.e., for imaging the topography and activity of single secretory cells [21]. Another way to use a shear-force feedback was seen in gluing the SECM tip to a tuning-fork resonance-detection system of a commercially available SNOM. The response of the tuning fork/SECM-tip assembly was used as a measure of shear-force induced damping of the tip vibration thus enabling a feedback control of tip-to-sample separation [22, 23]. Furthermore, an electrochemical impedance method for controlling the tip-to-sample distance during SECM experiments was proposed [24] and the integration of SECM into atomic force microscopes (AFM) by using specially-designed AFM cantilevers acting simultaneously as a force sensor for topographical AFM imaging and an ultramicroelectrode for electrochemical SECM imaging could be successfully demonstrated [26–32].

In a preceding article, we reported on a non-optical piezoelectric shear-force based constant-distance control for SECM tips [33]. The method was adapted to the specific needs of SECM from an earlier work by Brunner and Marti describing a similar approach for the positioning of SNOM tips [34, 35]. All important technical aspects of the set-up and the working principles allowing for the proper function of this new type of constant-distance mode SECM were described in detail and the performance of the method was proofed by imaging simultaneously the topography and local variations in the electrochemical activity of suitable samples. However, rather large, about 10 μm-diameter microelectrodes were used as SECM tips and, as a matter of fact, the spatial resolution was limited by their dimensions. In this article, we present our recent work on employing previously published Pt-disk nanoelectrodes [13] as miniaturized scanning probes for high-resolution SECM. We will give evidence that the accuracy and stability of the non-optical piezoelectric shear-force based distance control is suitable to allow for a precise positioning of nanometer-sized SECM tips not only in tip approach experiments but also throughout scanning. In fact, true SECM imaging with nanometer-sized SECM tips operated in the constant-distance mode will be shown for the first time and it will be demonstrated that a significant improvement in the spatial resolution of SECM imaging can be achieved when using nanoelectrodes as scanning probes.

2. Experimental

2.1. Chemicals, Samples, and SECM Tip Preparation

SECM experiments were carried out in aqueous solutions containing 5 mM $[Ru(NH_3)_6]Cl_3$ (Strem Chemicals, Newburyport, MA, USA) as the redox mediator and 0.5 M KCl (Riedel de Haen, Seelze, Germany) as supporting electrolyte. The sample studied was a three-dimensional microstructure with an array of hexagonal holes (honeycomb structure) (STEAG Microparts, Dortmund, Germany) prepared using the technique of deep X-ray lithography in combination with electroforming, also known as the LIGA (Lithographie, Galvanoformung, Abformung) microfabrication process [36]. SECM tips were glass-insulated Pt-disk nanoelectrodes prepared as previously described [13] by simultaneously pulling of a quartz glass capillary and an inserted platinum wire (25 μm in diameter, Goodfellow, Bad Nauheim, Germany) using a laser-based micropipette puller (Sutter P2000, Canada). Pulling typically produced two tapered glass tips with a Pt core of drastically reduced diameter tightly sealed into quartz glass. Careful polishing of the tips leads to the exposure of active Pt disks with diameters of far below one micrometer. For comparison reason, glass-insulated 10-μm-diameter Pt disk microelectrodes made from Pt wires (10 μm in diameter Goodfellow, Bad Nauheim, Germany) sealed into the tapered tips of pulled borosilicate glass capillaries have also been used as scanning probes [20].

2.2. Instrumentation, SECM Components

The design and the operational principles of the SECM set-up as used in this study for imaging with nanometer-sized SECM tips in a constant-distance mode of operation have been described earlier [33]. Experiments were usually carried out in a one-compartment electrochemical cell and three-electrode configuration, with the SECM tip (a Pt nano- or microelectrode) acting as working (WE), a Pt-wire as counter (CE) and a chlorinated silver wire as a Ag/AgCl pseudo-reference (RE) electrode.

3. Results and Discussion

Aiming on high resolution SECM imaging, needle-type Pt disk nanoelectrodes were integrated as extremely miniaturized SECM tips into the SECM set-up specially designed

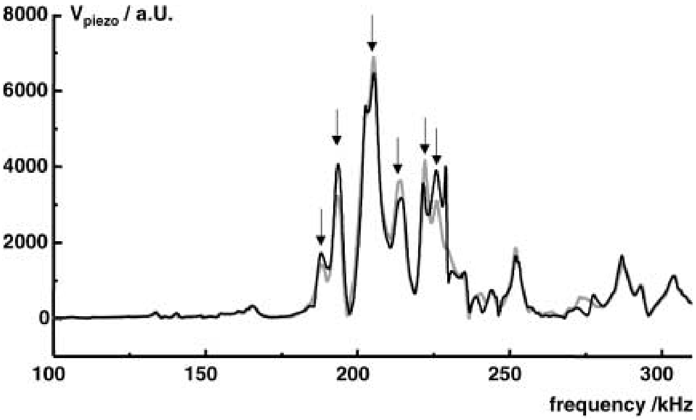

Fig. 1. Frequency spectra (V_{piezo}, the amplitude of the AC voltage from the detecting piezoelectric plate of the shear-force based distance control as measured with the lock-in amplifier as a function of the frequency of excitation applied to the agitation piezoelectric plate) obtained with the tip of a 450-nm-diameter Pt-disk nanoelectrode kept in air (solid gray line) and after being immersed into the electrolyte (solid black line). The arrows are indicating frequencies with significant differences in the response of the detecting piezoelectric plate, hence being connected with the damping of the vibration amplitude of the very end of the SECM tip.

for scanning in a constant-distance mode of operation. Before finally employed in SECM experiments, the electrochemical response of all Pt-disk nanoelectrodes was tested by cyclic voltammetry (CV) in solutions of 5 mM $[Ru(NH_3)_6]^{3+}$ containing 0.5 M KCl as background electrolyte and the obtained diffusion-limited currents were used to determine the actual diameter of the electroactive surface of the used nanoelectrode (CVs not shown, for representative CVs of these type of electrodes see [13]). Of note, the geometry of the tapered glass tips of the Pt nanoelectrodes with a typical length of about 15 mm and a very thin glass insulation for most of the pulled part of the apex gave them the appropriate mechanical properties to be used as flexible, vibrating SECM tips which are sensitive to the appearance of shear forces if brought into close proximity of a surface.

As already described previously, the key component of the SECM set-up with a non-optical, shear-force based constant-distance control is the integrated, piezoelectric shear-force detection system, which basically consists of two thin piezoelectric plates and two brass blocks. The brass blocks have a cylindrical hole drilled through their center from the top, just large enough in diameter to allow the SECM tip to be inserted and kept in place at various positions along the electrode body using a pair of small set screws. To complete the system, one of the piezoelectric plates was connected to a function generator allowing the application of small sinusoidal voltages in order to excite the SECM tip/brass holder assembly to vibration at resonance frequency. The second piezoelectric plate was connected to a lock-in amplifier and a phase-sensitive amplification of its alternating voltage was used to monitor the amplitude of the SECM tip oscillation.

With the tip of for instance a 450-nm-diameter Pt nanoelectrodes first kept in air and then immersed into the electrolyte, two frequency spectra (V_{piezo}, the amplitude of the AC voltage of the detecting piezo plate as measured with the lock-in amplifier as a function of the frequency of the voltage applied to the excitation piezo plate) were recorded and used to determine and choose resonance frequencies resulting from the vibration of the very end of the tip and hence being suitable to be applied with the piezoelectric shear force-based distance control. The arrows in Figure 1 indicate the resonance frequencies for the nanoelectrodes, and with values in the range of about 150 to 300 kHz they were found to be notably higher than the ones obtained for larger 10-μm-diameter Pt microelectrodes that typically displayed characteristic resonance frequencies from only 10 to 150 kHz [33]. The observed higher

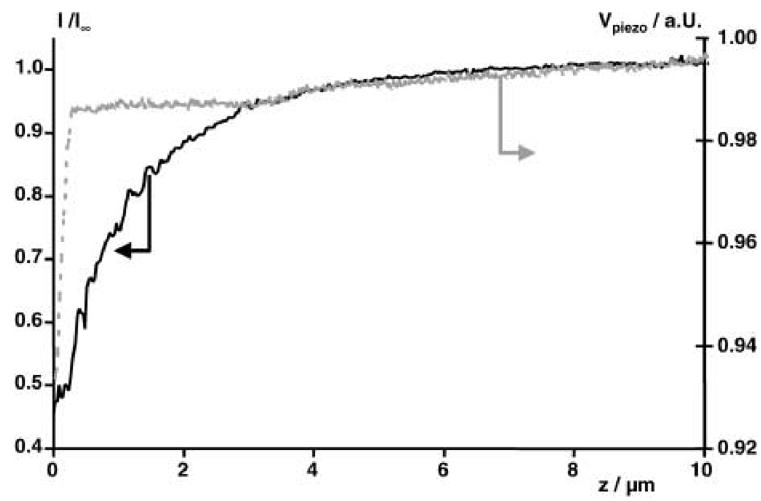

Fig. 2. Electrochemical and shear force-based approach curves obtained during the approach of a 450-nm-diameter Pt-disk nanoelectrode towards the insulating surface of a non-conductive glass surface. Measurements were performed in a solution containing 5 mM $[Ru(NH_3)_6]^{3+}$ and 0.5 M KCl with the nanoelectrode vibrating at 194 kHz and kept at −300 mV (vs. Ag/AgCl).

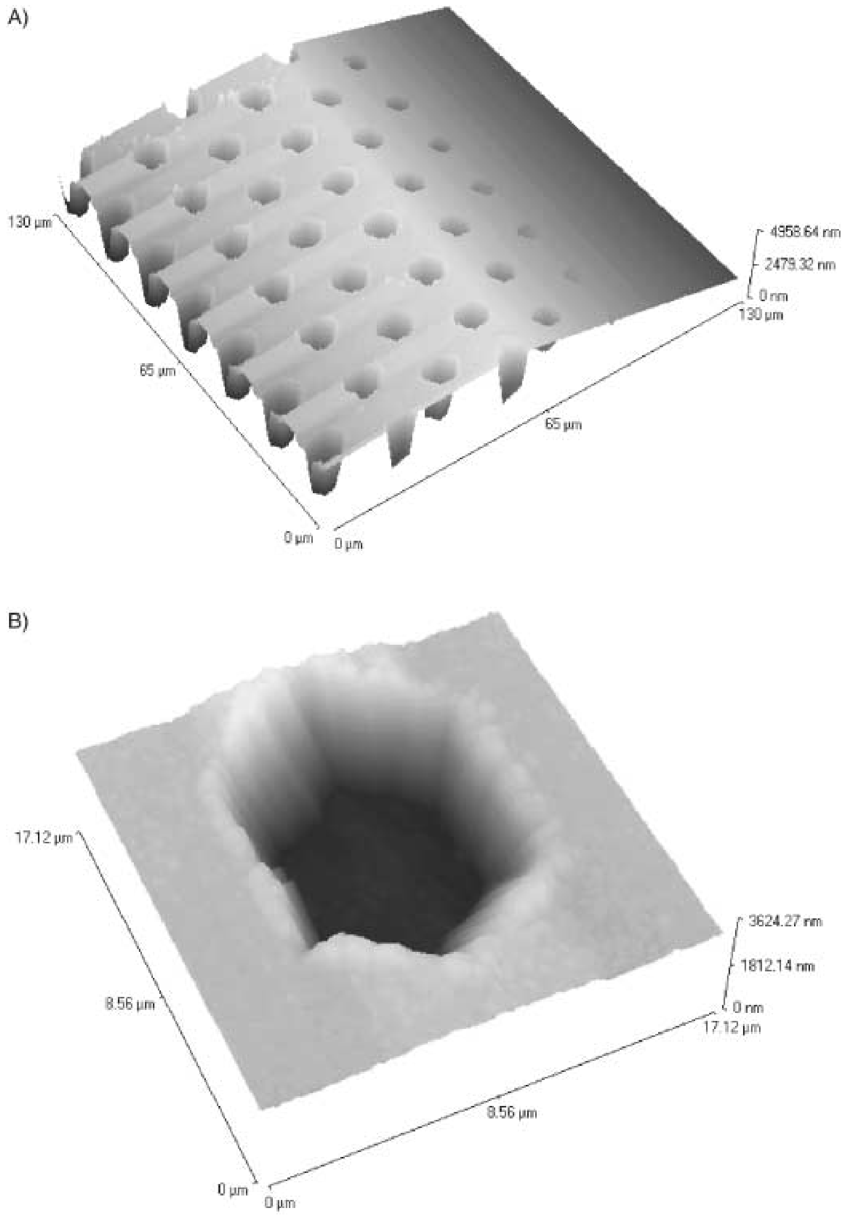

Fig. 3. Low (A) and high (B) resolution atomic force microscopy (AFM) images of the topography of the LIGA microstructure as used in this study as test sample.

resonance frequencies of the Pt nanoelectrodes might be explained by the differences in the type of glass used for tip insulation, the tip geometry and the thickness of the sealed Pt wires.

Shearforce-based approach curves were additionally done with nanoelectrodes with diameters down to about 100 nm, however, since both the positioning and the current measurements are becoming more difficult with decreasing electrode size, we have used the 450 nm electrode for all further experiments. In a first set of SECM experiments, electrochemical (amperometric SECM tip current vs. tip-to-sample distance *d*) and shear-force related (V_{piezo} vs. *d*) approach curves towards an insulating glass surface were simultaneously recorded in solutions of 5 mM $[Ru(NH_3)_6]^{3+}$ containing 0.5 M KCl with the chosen Pt nanoelectrode vibrating at an appropriate resonance frequency (i.e., at 194 kHz; derived from the frequency spectrum showed in Figure 1) and kept at a constant potential of -300 mV (vs. Ag/AgCl). As can be clearly seen in Figure 2, the two approach curves displayed the expected decrease in both, the tip current and the values of V_{piezo} giving a clear indication of the appearance of negative feedback and occurrence of shear force damping, respectively.

Prior to employing Pt-disk nanoelectrodes for imaging in the constant-distance mode of SECM, the computer-controlled feedback loop constantly regulating the tip-to-sample separation during scanning had to be established. This was done following the procedure as published earlier [33]. In brief, the Pt-disk nanoelectrode was brought to vibration at one of its shear-force sensitive resonance frequencies. Then, the tip of the nanoelectrode was moved slowly towards the sample surface while continuously monitoring V_{piezo}, the output of the lock-in amplifier. The z-approach was automatically stopped at a user-defined degree of damping of the vibration amplitude, usually at 70–80% of the unaffected value with the tip far above surface. The SECM software was used to determine the slope (dV_{piezo}/dz) at the very end of the approach curve, which then allowed setting the sensitivity of the closed-loop feedback control. Finally, a proper setting of a damping factor of the feedback regulation guaranteed that the feedback loop responded well to any change in the topography of the sample and that over swinging did not hinder successful imaging. Once the parameters of the feedback loop were defined, SECM imaging in the constant-distance mode of operation was performed at a speed of 0.1–1 $\mu m\ s^{-1}$ for x and y displacements while in the background the stable feedback loop continuously maintained a constant tip-to-sample distance of about 100–200 nm.

Imaging in the constant-distance mode of SECM was performed with either Pt-disk nanoelectrodes or, for comparison reason, a conventional-sized, 10-μm-diameter Pt-disk microelectrode on a three-dimensional gold LIGA microstructure with a regular pattern of hexagonal holes (honeycombs). Figure 3 shows low (A) and high (B) resolution atomic force microscopy (AFM) images of the topography of the polymer microstructure with the holes having a characteristic edge length of about 6 μm. Due to the convolution of the tip shape of the used cantilever with the holes only a depth of about 3–4 μm could be detected. However, the holes are going entirely through the LIGA structure that has a thickness of about 100 μm.

Figure 4 illustrates, respectively, the previously possible low-resolution topographical (A) and the current (B) images of a 100 μm × 100 μm area of the LIGA microstructure, simultaneously acquired by using the non-optical constant-distance mode SECM with a 10 μm diameter Pt-disk microelectrodes as SECM tip. In both images holes as present in the scanned area of the microstructure are visible. However, the spatial resolution of imaging was limited by the dimensions of the used microelectrode and therefore the quality of both the images was rather poor with neither the current nor the topography image displaying properly the details of the hexagonal honeycomb microstructure.

Changing the SECM tip and applying Pt-disk nanoelectrodes in the constant-distance mode of SECM for the visualization of the microscopic pattern of the LIGA microstructure offered a significant improvement in the quality of the SECM images. The beneficial effect of reducing the size of the SECM tip is presented in Figure 5 which shows the topographical (A: three-dimensional and B: top-view) and amperometric current (C) images of the LIGA microstructure as obtained by constant-distance mode SECM imaging with a vibrating 450 nm diameter Pt-disk electrode. In the topography images the hexagonal geometry of the holes through the microstructure is clearly recognizable. However, as already seen for the AFM tips, due to the thickness of the quartz-glass insulation of the Pt-nanoelectrodes the SECM tips are prevented to fully penetrate into the holes of the microstructure leading to the observed three-dimensional topography image. Because the holes are filled with the mediator-containing electrolyte, an increased diffusion of the redox active species towards the electroactive disk of the SECM tip was observed at positions just above the holes. This leads to an increase in the amperometric tip current exactly when the tip is positioned above these areas. The darker spots in the current image of the LIGA microstructure represent the areas at the sample surface with an increased tip current and they correspond very well with the holes as seen in the topography image which was measured at the same time.

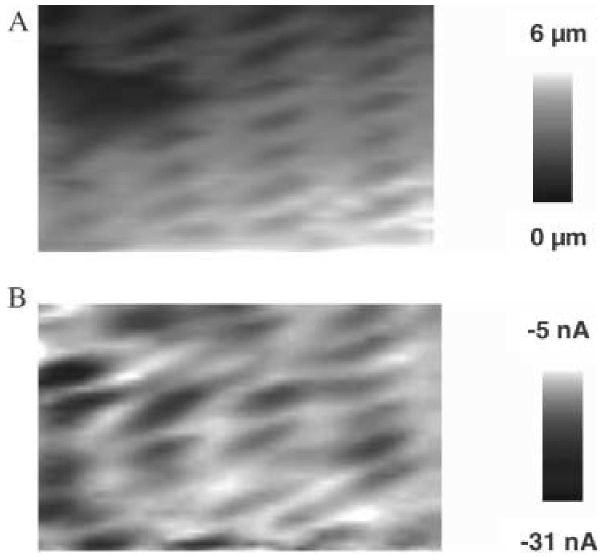

Fig. 4. Topographic (A) and amperometric feedback (B) images of a 100 μm × 100 μm portion of the LIGA microstructure. Both images were acquired simultaneously in a solution containing 5 mM $[Ru(NH_3)_6]^{3+}$ and 0.5 M KCl using a 10-μm-diameter Pt-disk microelectrode that was vibrating at resonance and kept at a constant working potential of −300 mV vs. Ag/AgCl while serving as the scanning tip for imaging with constant-distance mode SECM.

4. Conclusions

Pt disk nanoelectrodes were successfully applied as miniaturized SECM tips for high-resolution SECM imaging. Using a non-optical shear-force based distance control in a specially designed SECM set-up, an accurate and stable positioning of the Pt nanoelectrodes became possible not only in tip-approach experiments but also during SECM imaging. Obviously, the application of Pt nanoelectrodes as SECM probes lead to a significant improvement in the quality of the imaging resolution.

5. Acknowledgements

We gratefully acknowledge the financial support of this work by the Deutsche Forschungsgemeinschaft (DFG) in

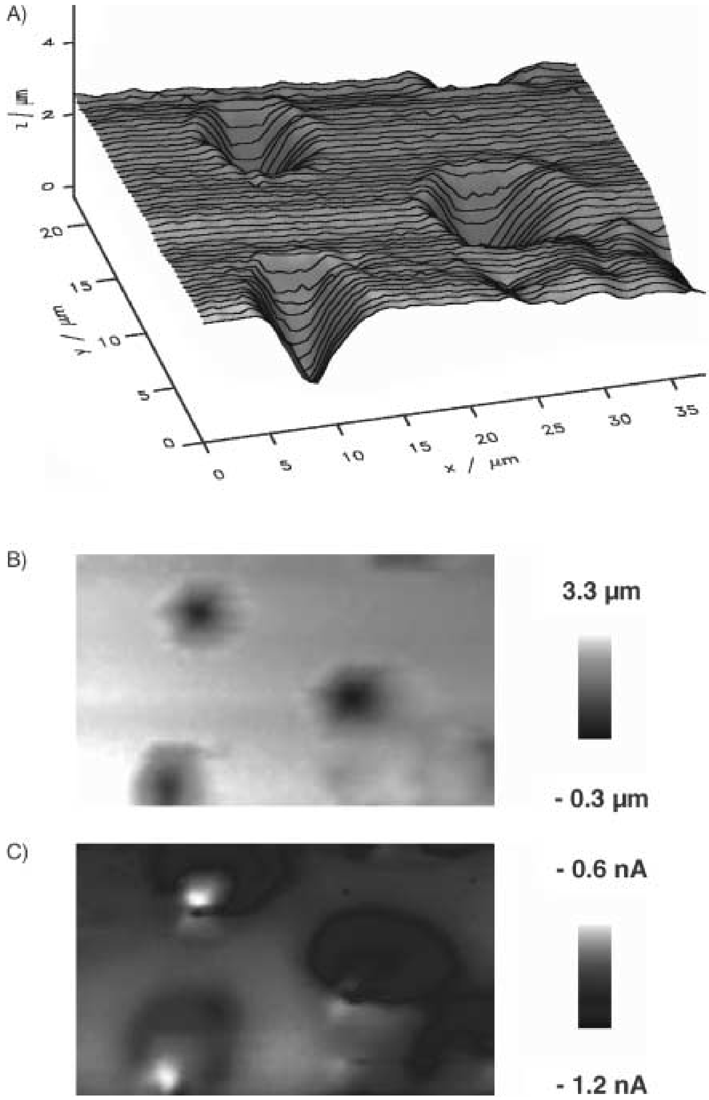

Fig. 5. Topographic (A: 3-D, B: top view) and amperometric feedback (C, top view) images of a 23 µm × 38 µm portion of the LIGA microstructure. The images were acquired all at once by constant-distance mode SECM carried out in a solution of 5 mM $[Ru(NH_3)_6]^{3+}$ containing 0.5 M KCl using a 450-nm-diameter Pt-disk nanoelectrode as the scanning probe (vibrating at resonance and kept at a constant potential of − 300 mV vs. Ag/AgCl).

the framework of the SFB 459, Project A5, and by the Ministry of Education and Research, Germany (BMBF) in the framework of its program "Nanobiotechnologie" (AZ NBT066).

6. References

[1] M. V. Mirkin, *Mikrochim. Acta* **1999**, *130*, 127.
[2] A. L. Barker, M. Gonsalves, J. V. Macpherson, C. J. Slevin, P. R. Unwin, *Anal. Chim. Acta* **1999**, *385*, 223.
[3] G. Nagy, L. Nagy, *Fresenius. J. Anal. Chem.* **2000**, *366*, 735.
[4] M. V. Mirkin, B. R. Horrocks, *Anal. Chim. Acta* **2000**, *406*, 119.
[5] G. Wittstock, *Fresen. J. Anal. Chem.* **2001**, *370*, 303.
[6] A. J. Bard, in: *Scanning Electrochemical Microscopy* (Eds: A. J. Bard, M. V. Mirkin), Marcel Dekker, New York **2001**, pp. 1 – 16.
[7] F. R. F. Fan, C. Demaille, in: *Scanning Electrochemical Microscopy* (Eds: A. J. Bard, M. V. Mirkin), Marcel Dekker, New York **2001**, pp. 75 – 110.
[8] C. Lee, C. J. Miller, A. J. Bard, *Anal. Chem.* **1991**, *63*, 78 – 83.
[9] Y. Shao, M. V. Mirkin, G. Fish, S. Kokotov, D. Palanker, A. Lewis, *Anal. Chem.* **1997**, *69*, 1627.
[10] J. K. Campbell, L. Sun, R. M. Crooks, *J. Am. Chem. Soc.* **1999**, *121*, 3779.
[11] C. J. Slevin, N. J. Gray, J. Macpherson, M. A. Webb, P. R. Unwin, *Electrochem. Comm.* **1999**, *1*, 282.
[12] P. Sun, Z. Zhang, J. Guo, Y. Shao, *Anal. Chem.* **2001**, *7*, 5346.
[13] B. Ballesteros Katemann, W. Schuhmann, *Electroanalysis*, **2002**, *14*, 22.
[14] D. W. Wipf, A. J. Bard, *Anal. Chem.* **1992**, *64*, 1362.
[15] K. Borgwarth, D. G. Ebling, J. Heinze, *Ber. Bunsenges. Phys. Chem.* **1994**, *98*, 1317.
[16] M. Ludwig, C. Kranz, W. Schuhmann, H. E. Gaub, *Rev. Sci. Instr.* **1995**, *66*, 2857.
[17] E. Betzig, J. K. Trautmann, T. D. Harris, J. S. Weiner, R. L. Kostelak, *Science*, **1991**, *251*, 1468.
[18] E. Betzig, P. L. Finn, J. S. Weiner, *Appl. Phys. Lett.* **1992**, *60*, 2484.
[19] C. Kranz, H. E. Gaub, W. Schuhmann, *Adv. Mater.* **1996**, *8*, 634.
[20] A. Hengstenberg, C. Kranz, W. Schuhmann, *Chem. Eur. J.* **2000**, *6*, 1547.
[21] A. Hengstenberg, A. Blöchl, I. D. Dietzel, W. Schuhmann, *Angew. Chem. Int. Ed. Engl.* **2001**, *5*, 905.
[22] P. I. James, L. F. Garfias-Mesias, P. J. Moyer, W. H. Smyrl, *J. Electrochem. Soc*. **1998**, *145*, L64.
[23] M. Büchler, S. C. Kelly, W. H. Smyrl, *Electrochem. Solid-State Lett.* **2000**, *3*, 35.
[24] M. A. Alpuche-Alviles, D. O. Wipf, *Anal. Chem*. **2001**, *73*, 4873.
[25] B. Ballesteros Katemann, A. Schulte, E. J. Calvo, M. Koudelka-Hep, W. Schuhmann. *Electrochem. Commun.* **2002**, *4*, 134.
[26] J. V. Macpherson, P. R. Unwin, *Anal. Chem.* **2000**, *72*, 276.
[27] C. Kranz, G. Friedbacher, B. Mizaikoff, *Anal. Chem.* **2001**, *73*, 2491.
[28] J. V. Macpherson, P. R. Unwin, *Anal. Chem.* **2001**, *73*, 550.
[29] A. Lugstein, E. Bertagnolli, C. Kranz, B. Mizaikoff, *Surf. Interface Anal.* **2002**, *33*, 146.
[30] J. V. Macpherson, J. P. G. de Mussy, J. L. Delplancke, *J. Electrochem. Soc.* **2002**, *149*, B306.
[31] J. V. Macpherson, C. E. Jones, A. L. Barker, P. R. Unwin, *Anal. Chem.* **2002**, *74*, 1841.
[32] C. E. Gardner, J. V. Macpherson, *Anal. Chem.* **2002**, *74*, 576A.
[33] B. Ballesteros Katemann, A. Schulte, W. Schuhmann, *Chem. Eur. J.* **2003**, *9*, 2025.
[34] R. Brunner, A. Bietsch, O. Hollricher, O. Marti, *Rev. Sci. Instrum*. **1997**, *68*, 1769.
[35] O. Hollricher, R. Brunner, O. Marti, *Ultramicroscopy*, **1998**, *71*, 143.
[36] W. Ehrfeld, A. Schmidt, *J. Vac. Sci. Techn. B*, **1998**, *16*, 3526.